200 Gb/s Optical-Amplifier-Free IM/DD Transmissions Using a Directly Modulated O-Band DFB+R Laser Targeting LR Applications

Xiaodan Pang, *Senior Member, IEEE*, Toms Salgals, Hadrien Louchet, Di Che, Markus Gruen, Yasuhiro Matsui, Thomas Dippon, Richard Schatz, Mahdieh Joharifar, Benjamin Krüger, Fabio Pittala, Yuchuan Fan, Aleksejs Udalcovs, *Senior Member, IEEE*, Lu Zhang, Xianbin Yu, *Senior Member, IEEE*, Sandis Spolitis, *Member, IEEE*, Vjaceslavs Bobrovs, Sergei Popov, and Oskars Ozolins, *Senior Member, IEEE*

***Abstract*—We experimentally demonstrate an O-band single-lane 200 Gb/s intensity modulation direct detection (IM/DD) transmission system using a low-chirp, broadband, and high-power directly modulated laser (DML). The employed laser is an isolator-free packaged module with over 65-GHz modulation bandwidth enabled by a distributed feedback plus passive waveguide reflection (DFB+R) design. We transmit high baud rate signals over 20-km standard single-mode fiber (SSMF) without using any optical amplifiers and demodulate them with reasonably low-complexity digital equalizers. We generate and detect up to 170 Gbaud non-return-to-zero on-off-keying (NRZ-OOK), 112 Gbaud 4-level pulse amplitude modulation (PAM4), and 100 Gbaud PAM6 in the optical back-to-back configuration. After transmission over the 20-km optical-amplifier-free SSMF link, up to 150 Gbaud NRZ-OOK, 106 Gbaud PAM4, and 80 Gbaud PAM6 signals are successfully received and demodulated, achieving bit error rate (BER) performance below the 6.25%-overhead hard-decision (HD) forward-error-correction code (FEC) limit. The demonstrated results show the possibility of meeting the strict requirements towards the development of 200 Gb/s/lane IM/DD technologies, targeting 800 Gb/s and 1.6 Tb/s LR applications.**

***Index Terms*—Direct modulation, distributed-feedback laser, on-off keying, pulse amplitude modulation.**

Manuscript received 21 December 2022; revised 17 February 2023; accepted 22 March 2023. Date of publication 24 March 2023; date of current version 9 June 2023. This work was supported in part by the H2020 ICT TWILIGHT Project under Grant 781471, in part by the Swedish Research Council (VR) Projects under Grant 2019-05197, in part by BRAIN Project under Grant 2022-04798, in part by RTU Science Support Fund, in part by the ERDF-Funded RINGO Project under Grant 1.1.1.1/21/A/052, and in part by the National Key Research and Development Program of China under Grant 2018YFB1801503. *(Corresponding authors: Xiaodan Pang; Oskars Ozolins.)*

Xiaodan Pang is with the Department of Applied Physics, KTH Royal Institute of Technology, 106 91 Stockholm, Sweden, with the RISE Research Institutes of Sweden, 164 40 Kista, Sweden, and also with the Institute of Telecommunications, Riga Technical University, 1048 Riga, Latvia (e-mail: xiaodan@kth.se).

Richard Schatz, Mahdieh Joharifar, and Sergei Popov are with the Department of Applied Physics, KTH Royal Institute of Technology, 106 91 Stockholm, Sweden (e-mail: rschatz@kth.se; madieh@kth.se; sergeip@kth.se).

Vjaceslavs Bobrovs is with the Institute of Telecommunications, Riga Technical University, 1048 Riga, Latvia (e-mail: vjaceslavs.bobrovs@rtu.lv).

Oskars Ozolins is with the Department of Applied Physics, KTH Royal Institute of Technology, 106 91 Stockholm, Sweden, with the Institute of Telecommunications, Riga Technical University, 1048 Riga, Latvia, and also with the RISE Research Institutes of Sweden, 164 40 Kista, Sweden (e-mail: oskars.ozolins@ri.se).

Toms Salgals and Sandis Spolitis are with the Institute of Telecommunications, Riga Technical University, 1048 Riga, Latvia, and also with the Communication Technologies Research Center, Riga Technical University, 1048 Riga, Latvia (e-mail: toms.salgals@rtu.lv; sandis.spolitis@rtu.lv).

Hadrien Louchet, Markus Gruen, Thomas Dippon, Benjamin Krüger, and Fabio Pittala are with the Keysight Technologies GmbH, 71034 Böblingen, Germany (e-mail: hadrien.louchet@keysight.com; markus.gruen@keysight.com; thomas_dippon@keysight.com; benjamin.krueger@keysight.com; fabio.pittala@keysight.com).

Di Che is with the Nokia Bell Labs, Murray Hill, NJ 07974 USA (e-mail: di.che@nokia-bell-labs.com).

Yasuhiro Matsui is with the Coherent Incorporation, Fremont, CA 94538 USA (e-mail: yasuhiro.matsui@ii-vi.com).

Yuchuan Fan and Aleksejs Udalcovs are with the RISE Research Institutes of Sweden, 164 40 Kista, Sweden (e-mail: yuchuan.fan@ri.se; aleksejs.udalcovs@gmail.com).

Lu Zhang and Xianbin Yu are with the College of Information Science and Electronic Engineering, Zhejiang University, Hangzhou 310058, China, and also with the Zhejiang Lab, Hangzhou 311121, China (e-mail: zhanglu1993@zju.edu.cn; xyu@zju.edu.cn).

Color versions of one or more figures in this article are available at https://doi.org/10.1109/JLT.2023.3261421.

Digital Object Identifier 10.1109/JLT.2023.3261421

I. Introduction

DRIVEN by the rapid traffic growth and the subsequent bandwidth-scaling pace of switches for data center networks, the technology roadmap indicates the upgrade from the ongoing-deployed 400 Gb/s optical modules to the next-generation 800 Gb/s or 1.6 Tb/s optical modules, will soon happen. Consequently, upgrading the single-lane data rates from 100 Gb/s to 200 Gb/s will be desirable to reduce the lane count and footprint [1]. Compared with 50/100 Gb/s lane rates, the 200 Gb/s/lane technologies face both fundamental and practical challenges towards development, including system bandwidth limitation from both the electronics and optoelectronics, limited footprint and energy efficiency from the components, and the digital signal processing (DSP) application-specific integrated circuit (ASIC), as well as the bounded latency requirement from the forward error correction (FEC) coder and decoder [2]. Moreover, the power budget requirements become very stringent, and the power penalties induced by chromatic dispersion (CD) become non-negligible on the side channels of the 20-nm spacing 4-channel coarse wavelength division multiplexing (CWDM4) or even the 800-GHz spacing LAN-WDM4 configurations. Therefore, it is more likely to firstly extend the intensity-modulation and direct-detection (IM/DD) technologies to DR

(500 m) or DR+ (2 km) coverage at 200 Gb/s/lane with parallel single mode fiber (PSM) configurations. Further extending the IM/DD technologies to support FR (2 km CWDM4) and even LR applications (6 km/10 km LAN-WDM4) becomes exceptionally challenging considering the required power budget to compensate for the CD-induced power penalties and therefore remains to be explored [3].

In recent years, many 200 Gb/s/lane IM/DD transmissions have been demonstrated using different types of enabling broadband optoelectronic components [4]. On the one hand, external modulator-based transmitters such as silicon-photonic [5], [6], plasmonic [7], [8], [9], and thin-film Lithium Niobate- (TFLN) [10], [11], [12], [13] Mach-Zehnder modulators (MZM) or micro-ring modulators (MRM) [14], [15], [16] have shown excellent performance in terms of bandwidth and modulation linearity for high baud rate operation, however, requiring high-power external light sources to operate. On the other hand, monolithically integrated transmitters such as electro-absorption modulated lasers (EML) [17], [18], [19], [20], [21], [22], [23], [24], [25] and directly modulated lasers (DML) [26], [27], [28], [29], [30], [31] with a potentially smaller footprint and lower power consumption, also show promising characteristics in supporting over 200 Gb/s/lane transmissions. Moreover, recent efforts in monolithically integrating laser sources with TFLN modulators have been reported [32].

However, most of these reported over 200 Gb/s IM/DD transmission results are achieved with the assistance of optical amplifiers or complex DSP algorithms, particularly for transmission distances over 10 km. Digital equalizers of over a few tens or even hundreds of taps, complex nonlinear equalizers based on 2nd or 3rd-order Volterra series, or artificial neural networks (ANN) are often employed to combat the bandwidth (BW) limit and other linear/nonlinear system impairments. Moreover, many of these demonstrations were benchmarked against the high-coding gain soft/hard-decision (SD/HD) FEC code limit with large overhead (OH). Although the use of concatenated SD-FEC schemes has recently been discussed in IEEE 802.3 to improve the overall coding gain [33], it also suggests that large OH should be avoided, as it may introduce unrealistically high complexity and latency for datacom applications. Concatenated FEC framework was proposed by the 800G Pluggable MSA to adopt staircase code variants for FR specification, which appears as a reasonable option considering the balance between coding gain and latency [34]. As we are approaching standardization and practical development, it is extremely challenging to simultaneously meet the stringent requirements of high-bandwidth and sufficient power budget while maintaining low cost, low complexity, and low latency. Lately, several vendors have reported and demonstrated 200 Gb/s EML modules, mainly targeting DR/DR+ and FR applications, and their capabilities in supporting LR applications remain to be seen [35], [36], [37]. Meanwhile, it's worth mentioning that a state-of-the-art 200 Gb/s transmission system demonstration using a high-power DFB+R laser was reported, achieving 10-km single-mode fiber (SMF) with 800G compliant DSP, achieving bit error rate (BER) performance below 7% HD-FEC limit [31]. Yet, the system-level performance limit of such lasers remained to be further explored with higher-speed electronics and longer transmission distances.

In this article, we extend our latest report on a 200 Gb/s O-band optical-amplifier-free IM/DD system using a directly modulated DFB+R laser [38], with additional results of higher baud rate signals generation and detection in the optical back-to-back configuration and more detailed discussions. Compared with the previous demonstration with the DFB+R [31], this time, we further improved on the generated and received signal quality by using higher sampling-rate test equipment, i.e., arbitrary waveform generator (AWG, Keysight M8199A) and real-time digital storage oscilloscope (DSO, Keysight UXR1104A) both operating at 256 GSa/s and carefully optimized impedance matching at all connections. We show that the demonstrated system can meet the strict requirements of the power budget of 20-km standard single-mode fiber (SSMF) transmission without the use of any high-complexity nonlinear digital equalizations, achieving BER performance below the 6.25%-overhead (OH) hard-decision (HD)-FEC limit [39]. Note that the adopted FEC limit is only for the purpose of benchmarking the system performance whereas the practical FEC implementation for the targeted scenarios remains to be defined. This work, to the best of our knowledge, is among the first experimental demonstrations of 200 Gb/s optical-amplifier-free IM/DD systems simultaneously fulfilling these practical requirements, carrying on the momentum of developing high-baud rate IM/DD solutions for 800 Gb/s or 1.6 Tb/s for LR applications.

II. Experimental Configuration

In this section, we first introduce the key enabling components of the high-speed transmission demonstration, i.e., the high bandwidth directly modulated DFB+R laser module. Then, we briefly describe its features and show the measured characteristics. Next, we describe the experimental configuration of the transmission system in detail, enabled both by this laser module and the state-of-the-art high-speed testing equipment.

A. Low-Chirp Broadband DFB+R Laser

In this experiment, the enabling component is a packaged 65-GHz-class DFB+R laser module with low chirp and high output power, which was fabricated on a time-tested reliable InP buried heterostructure (BH) platform based on a recently reported design [30]. A photo of the laser module is shown in Fig. 1(a). In this design, two essential effects are utilized to enhance the modulation performance of the laser, i.e., the photon-photon resonance (PPR) effect [40] and the detuned-loading (DL) effect [41]. For the PPR, a passive waveguide is integrated with the DFB laser to provide optical feedback to the DFB section, forming an external cavity mode in the vicinity of the DFB mode that resonantly amplifies the modulation sideband of the DFB laser, thus enhancing the modulation bandwidth. The DL effect is realized by forming an in-cavity etalon filter between the DFB grating and a 3% mirror on the facet of the passive waveguide, enhancing the differential gain and reduces the laser chirp. Consequently, the modulation bandwidth is improved.

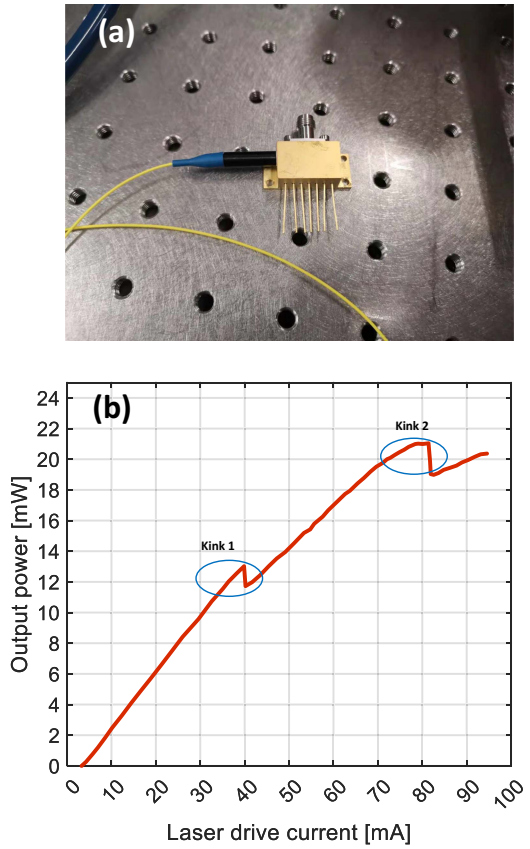

Fig. 1. (a) A photo of the packaged directly modulated DFB+R laser module. (b) The measured P-I curve of the laser, where two kink points are observed where mode hops occur.

The P-I curve of the DFB+R laser is shown in Fig. 1(b), which was measured when operating at 17 °C. Two kink points are observed with increased laser drive current where the output power drops due to mode hops. Both the DL and the PPR effects are maximized before the kink points. Thus, the laser is optimally operated close to the kink points to maximize the modulation bandwidth. In the experiment, optimal bias points were found around 8-9 mA before the kinks, as biasing the laser too close to the kinks may cause instability and lead to unwanted mode hops. Therefore, in practical transceiver configurations where automatic power control is required, it is advisable to use an external power regulator and avoid regulating the power by adjusting the laser bias. It is worth noting that more than 20 mW output power can be obtained when driving the laser at the optimal operating point close to kink 2.

B. Optical Amplifier-Free IM/DD Transmission Setup

Fig. 2 shows the experimental setup for the IM/DD transmission system. We use a 256 GSa/s AWG of 65 GHz bandwidth to generate the modulation signals. Three modulation formats are employed for system performance evaluation, i.e., non-return-to-zero on-off-keying (NRZ-OOK), 4-level pulse amplitude modulation (PAM4), and PAM6. Their symbols are Gray coded from a random binary sequence of >1 million unrepeated bit-length generated using the Mersenne Twister with a shuffled seed number. Then, the symbol sequence is filtered with a root-raised-cosine (RRC) pulse shaping filter with roll-off factors of between 0.1 and 0.2, optimized for different baud rates and each modulation format. The AWG output signal is amplified to around 2 Vpp by an electrical amplifier (EA) of 65 GHz. An external bias-tee with 60-GHz bandwidth is used to deliver the combined bias current and the modulation signal to the DFB+R laser. The operational temperature of the laser is stabilized at 17 °C with a thermoelectric controller (TEC). One should note that it is possible to achieve a cavity-enhanced DML bandwidth also at a higher temperature, e.g., 50 °C, under semi-cool operation to reduce TEC power consumption. However, such an operation may introduce slightly degraded performance in terms of bandwidth and power due to the thermal reduction of the material differential gain. Such a degradation should be practically compensated for by improved driving signal quality and higher modulation depth when developing the transceiver. The DFB+R output is directly launched into a 20-km G.652 SSMF link. At the receiver, the received optical power (ROP) is adjusted by a variable optical attenuator (VOA) and detected by a 70 GHz photodiode (PD). After the PD, the signal is electrically amplified by another 65-GHz EA and captured by a 256 GSa/s real-time DSO with 110 GHz bandwidth. No optical amplifiers are used before or after the fiber transmission. For offline demodulation, the received signal is firstly upsampled to 8 samples per symbol and then decimated to 1 sample per symbol based on the maximum variance method. Then symbol-spaced data-aided feedforward equalizers (FFE) or decision feedback equalizers (DFE) are employed for equalization. The equalizers are trained with the first 2^{13} symbols for convergence. After convergence, the equalizers are tested on the remaining sequences of >1 million symbols with blind adaptation. After equalization, hard decisions are performed on the symbols for symbol-to-bit demodulation, and the BER is counted for each modulation format.

Fig. 3(a) and (b) show the characterized end-to-end amplitude and phase response of the system in an optical back-to-back (B2B) configuration, including the cascaded channel responses of the AWG, the DFB+R laser, the PD, the DSO, and all the electrical components in between, measured close to the two kink points, respectively. A more flattened amplitude response and a smoother phase response are observed when biasing the laser close to kink 2 compared with biasing at kink 1. Moreover, the DFB+R laser has almost 3 dB higher output power when biasing around kink 2 than kink 1, as earlier shown in Fig. 1. Therefore, the bias point of the laser was set close to kink 2 at around 71 mA during the transmission measurements to obtain an optimal balance between bandwidth and stability. Finally, based on the pre-calibrated amplitude and phase responses shown in Fig. 3, we perform static pre-equalization at the AWG to flatten the response up to 45 GHz.

Fig. 4 shows the optical spectra of the optical signals measured after the 20-km SSMF link, modulated with signals of three modulation formats at different baud rates when the laser is biased at 71 mA. The central wavelength of the DFB+R laser at this bias point is around 1313.8 nm.

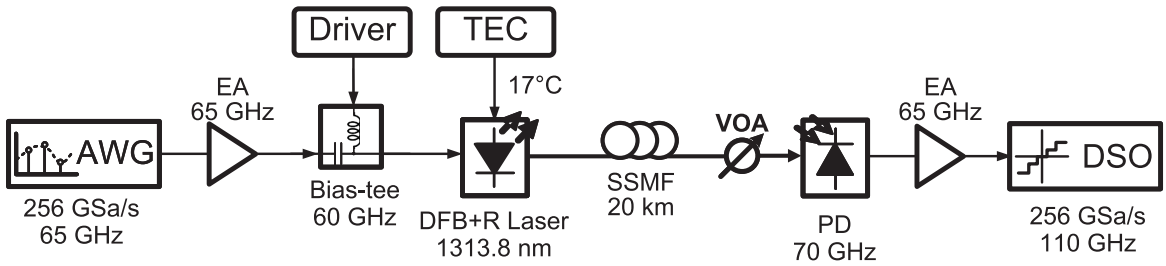

Fig. 2. The experimental setup of the DML-based IM/DD transmission link. AWG: Arbitrary waveform generator. EA: Electrical amplifier. TEC: Thermoelectric controller. SSMF: Standard single-mode-fiber. VOA: Variable optical attenuator. PD: Photodiode. DSO: Digital storage oscilloscope.

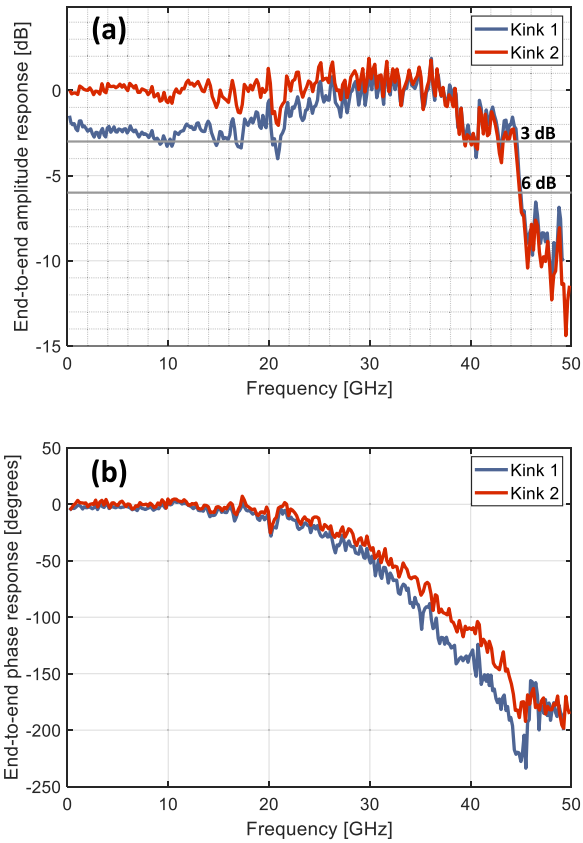

Fig. 3. The end-to-end system frequency responses of (a) the amplitude and (b) the phase measured at two kink points, respectively. Measurements were performed with the optical B2B configuration without the fiber link.

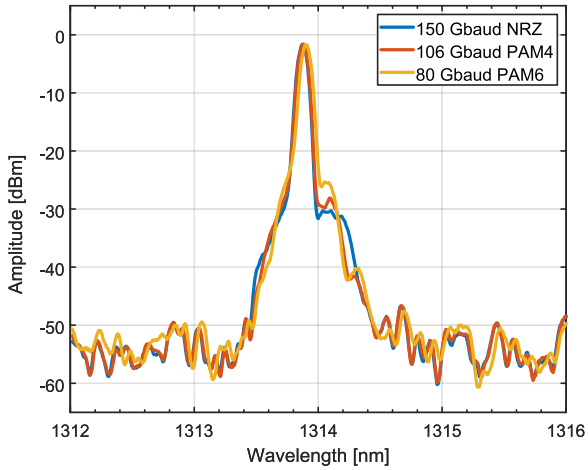

Fig. 4. Optical spectra of received signals measured after the 20-km SSMF transmissions for the three evaluated modulation formats with different baud rates.

III. Experimental Results

After characterizing the power and frequency performance of the DFB+R laser, we continue with evaluating the system transmission performance with the previously mentioned three modulation formats, i.e., NRZ-OOK, PAM4, and PAM6. For each modulation format under test, we explore the highest bit rates with achievable BER against the 6.25%-OH staircase HD-FEC limit of 4.5E-3 [39]. One should note that such an FEC threshold is only adopted for performance benchmarking, and more specific FEC codes should be applied in practice. Moreover, the complexity of the digital equalizers is bounded to symbol-spaced FFE or DFE with a total number of taps below 50 to emulate the performance of practically implementable configurations.

A. Transmission Performance of NRZ-OOK

Fig. 5(a) shows the BER performance as a function of the received optical power for 150 Gbaud NRZ-OOK, which is the highest achievable baud rate after transmission over 20-km SSMF. In this case, due to the significant inter-symbol interference (ISI) induced by the bandwidth limit of the system, BER floors above the 6.25%-OH HD-FEC limit are observed when equalized only with FFE of up to 33 taps, as the FFE enhances the high-frequency noise. In all cases, clear performance improvements are observed when adding only 3 decision feedback taps. We show that 13-tap FFE + 3-tap DFE is sufficient to compensate for the ISI and suppress the high-frequency noise enhancement to achieve BER performance below the KR4-FEC threshold of 2×10^{-5} in the B2B case and below the 6.25%-OH HD-FEC threshold after 20-km SSMF transmission. Moreover, negligible power penalty is observed with the fiber transmission, as the laser wavelength is close to the zero dispersion point of the SSMF.

We further explore the highest achievable NRZ-OOK baud rate only in the optical B2B configuration. In this case, up to 170 Gbaud signal is successfully generated and received, and the results are shown in Fig. 5(b). Due to the increased signal

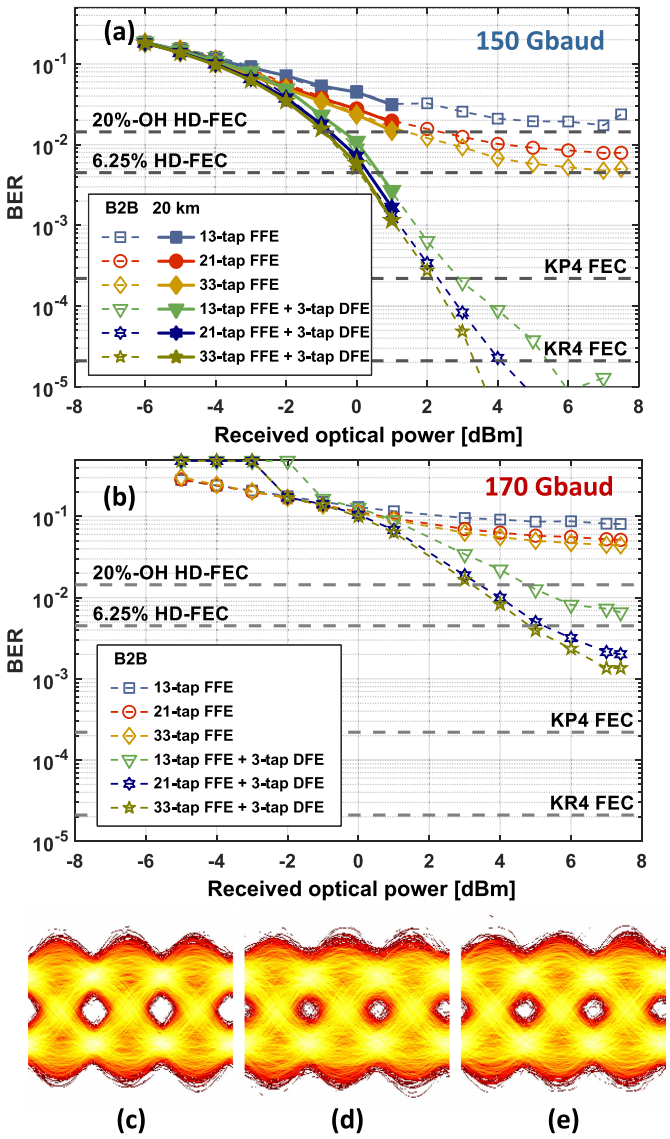

Fig. 5. Measured BER results as a function of the received optical power for (a) 150 Gbaud NRZ in both the optical B2B and 20-km SSMF cases, and (b) 170 Gbaud NRZ for optical B2B, respectively, with different FFE/DFE configurations. Selected eye diagrams are shown for the cases of (c) 150 Gbaud B2B, (d) 150 Gbaud 20-km SSMF and (e) 170 Gbaud B2B measured after 33-tap FFE+3-tap DFE at highest received optical power, respectively.

bandwidth and the subsequent more severe ISI, up to 21-tap FFE + 3-tap DFE is required to achieve BER performance below the 6.25%-OH HD-FEC threshold. We also observed signal demodulation failures at low received optical power values (<-2 dBm) in the case of using DFE, as shown in Fig. 5(b), resulting from severe error propagation. Fig. 5(c), (d), and (e) show selected eye diagrams for the 150 Gbaud NRZ-OOK signals in both the optical B2B and after 20-km SSMF cases, as well as the 170 Gbaud NRZ-OOK in the optical B2B case. The eye diagrams are plotted after 33-tap FFE+3-tap DFE at the respective highest received optical power value for each case. Clear eye openings can be observed in all three cases.

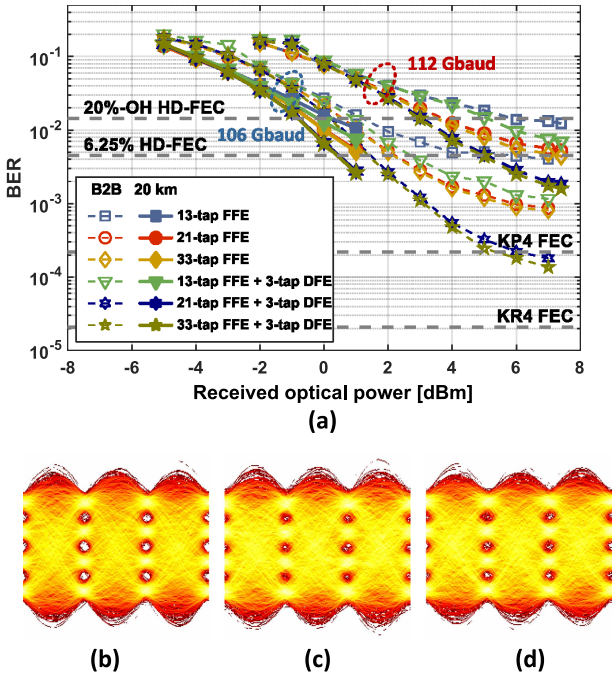

Fig. 6. (a) Measured BER results as a function of the received optical power for 106 Gbaud PAM4 in both the optical B2B and 20-km SSMF cases, and 112 Gbaud PAM4 for optical B2B, respectively, with different FFE/DFE configurations. Selected eye diagrams are shown for the cases of (b) 106 Gbaud B2B, (c) 106 Gbaud after 20-km SSMF and (d) 112 Gbaud B2B measured after 33-tap FFE+3-tap DFE at highest received optical power, respectively.

B. Transmission Performance of PAM4

We then switch to the PAM4 signal format with the same system configuration to explore the supported data rates against the benchmarking FEC threshold. For PAM4, we achieved up to 106 Gbaud symbol rate after the 20-km SMF, corresponding to a gross data rate of 212 Gb/s. Fig. 6(a) shows the measured BER results with different equalizer configurations. Compared with the NRZ-OOK, the performance gap between the FFE-only and the FFE+DFE cases becomes smaller due to reduced signal bandwidth. Thus, the impact of the DFE taps becomes less significant as the FFE-induced high-frequency noise enhancement is reduced. Nevertheless, the decision feedback taps are still necessary to achieve the below FEC threshold performance. With 21-tap FFE + 3-tap DFE, the BER can reach below the KP4-FEC limit of 2.2×10^{-4} for optical B2B and below the 6.25%-OH HD-FEC threshold after 20-km SSMF transmission. Again, we explore the highest achievable symbol rate only with optical B2B, showing that 112 Gbaud PAM4 can be generated and received with a BER floor below the 6.25%-OH HD-FEC threshold. Selected eye diagrams for the three cases are shown in Fig. 6(b)–(d), respectively. These eye diagrams show that the DFB+R laser is driven within its linear modulation region with no eye compressions in the upper or lower amplitude levels observed.

C. Transmission Performance of PAM6

Lastly, the transmission performance of PAM6 is evaluated with the experimental setup. Up to 100 Gbaud and 80 Gbaud

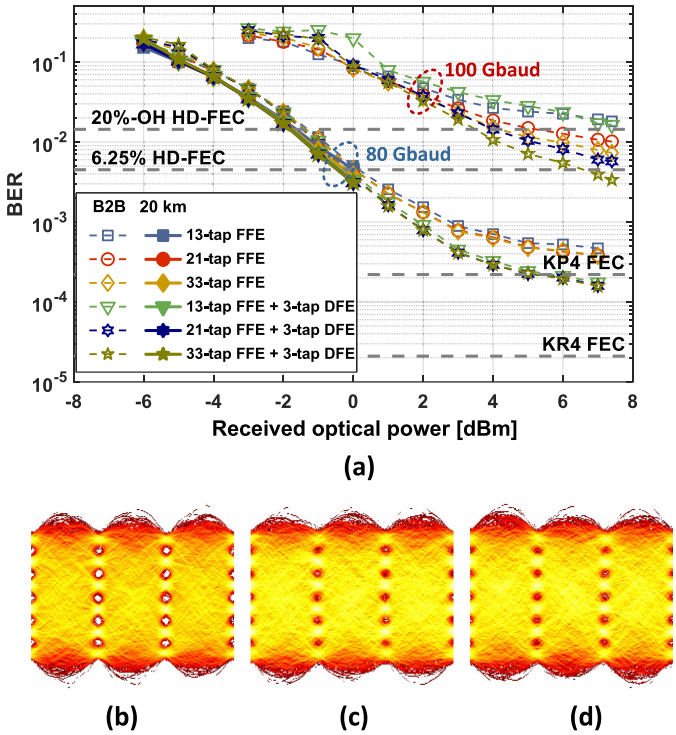

Fig. 7. (a) Measured BER results as a function of the received optical power for 80 Gbaud PAM6 in both the optical B2B and 20-km SSMF cases, and 100 Gbaud PAM6 for optical B2B, respectively, with different FFE/DFE configurations. Selected eye diagrams are shown for the cases of (b) 80 Gbaud B2B, (c) 80 Gbaud after 20-km SSMF and (d) 100 Gbaud B2B measured after 33-tap FFE+3-tap DFE at highest received optical power, respectively.

are achieved in optical B2B and after 20-km SSMF cases, corresponding to gross data rates of 250 Gb/s and 200 Gb/s, respectively. Fig. 7(a) shows the measured BER results. At 80 Gbaud, 13-tap FFE + 3-tap DFE is needed to achieve BER performance below the KP4 FEC limit for optical B2B, and only 13-tap FFE is required to achieve below the 6.25%-OH HD-FEC limit after 20-km SSMF transmission. The performance gap between the FFE-only and the FFE+DFE cases becomes even smaller, and they almost overlap with each other at the highest received optical power after the 20-km SSMF transmission. This is due to the reduced signal bandwidth, resulting in decreased high-frequency noise enhancement after the FFE. At 100 Gbaud, at least 33-tap FFE + 3-tap DFE is required to achieve BER below the 6.25%-OH HD-FEC threshold in the case of optical B2B.

Fig. 7 also shows the selected eye diagrams for all tested cases at their highest received optical power, respectively. Again, excellent modulation linearity and noise characteristics of the directly modulated DFB+R laser are verified as there are no amplitude compressions at high-level modulation formats, despite that no nonlinear equalizers are employed.

In summary, up to 200 Gb/s IM/DD transmission over 20-km SSMF can be achieved with both PAM4 and PAM6 signals. It is worth noting that we demonstrate 20-km transmission with the purpose of showing power budget margins to potentially compensate for the power penalties of the side channels in CWDM4 or LAN-WDM4 configurations in supporting 6 km or 10 km LR applications. The actual implementation of WDM with multiple DFB+R lasers with dedicated wavelengths will be the next-phase target.

IV. Conclusion

We experimentally demonstrate up to 200 Gb/s IM/DD transmissions over 20-km SSMF in the O-band without using any optical amplifiers or complex nonlinear digital equalizers, benchmarked against the 6.25%-OH HD-FEC limit. The key enabling component is the high-power, low-chirp, and broadband directly modulated DFB+R laser. We show that the modulation and power characteristics of the tested laser module can potentially support 200 Gb/s/lane IM/DD transmission for 6 km or 10 km LR applications, which are considered highly challenging with other types of integrated optical transmitters without the use of optical amplifications. We consider this demonstration a solid case for carrying on the momentum of IM/DD technologies for the next-generation 800 Gb/s or 1.6 Tb/s data center applications.

Acknowledgment

We thank Keysight Technologies for loaning the M8199A Arbitrary Waveform Generator and the UXR1104A Infiniium UXR-Series Oscilloscope.

References

[1] "IEEE P802.3df 200 Gb/s, 400 Gb/s, 800 Gb/s, and 1.6 Tb/s Ethernet TaskForce," 2022. Accessed: Dec. 19, 2022. [Online]. Available: https://www.ieee802.org/3/df/index.html

[2] M. Spyropoulou et al., "The path to 1Tb/s and beyond datacenter interconnect networks: Technologies, components, and subsystems," *Proc. SPIE*, vol. 11712, 2021, Art. no. 117120G.

[3] X. Pang et al., "Short reach communication technologies for client-side optics beyond 400 Gbps," *IEEE Photon. Technol. Lett.*, vol. 33, no. 18, pp. 1046–1049, Sep. 2021.

[4] X. Pang et al., "200 Gbps/lane IM/DD technologies for short reach optical interconnects," *J. Lightw. Technol.*, vol. 38, no. 2, pp. 492–503, Jan. 2020.

[5] M. S. Alam et al., "Net 220 Gbps/λ IM/DD transmission in O-band and C-band with silicon photonic traveling-wave MZM," *J. Lightw. Technol.*, vol. 39, no. 13, pp. 4270–4278, Jul. 2021.

[6] M. S. Alam, X. Li, M. Jacques, E. Berikaa, P.-C. Koh, and D. V. Plant, "Net 300 Gbps/λ transmission over 2 km of SMF with a silicon photonic Mach-Zehnder modulator," *IEEE Photon. Technol. Lett.*, vol. 33, no. 24, pp. 1391–1394, Dec. 2021.

[7] W. Heni et al., "Ultra-high-speed 2:1 digital selector and plasmonic modulator IM/DD transmitter operating at 222 GBaud for intra-datacenter applications," *J. Lightw. Technol.*, vol. 38, no. 9, pp. 2734–2739, May 2020.

[8] H. Sato, J. Mao, A. Bannaron, T. Kamiya, G.-W. Lu, and S. Yokoyama, "A 100 Gbaud on-off-keying silicon-polymer hybrid modulator operating at up to 110 °C," *IEEE Photon. Technol.*, vol. 33, no. 24, pp. 1507–1510, Dec. 2021.

[9] Q. Hu et al., "Ultrahigh-net-bitrate 363 Gbit/s PAM-8 and 279 Gbit/s polybinary optical transmission using plasmonic Mach-Zehnder modulator," *J. Lightw. Technol.*, vol. 40, no. 10, pp. 3338–3346, May 2022.

[10] D. Che and X. Chen, "Higher-order modulation vs faster-than-Nyquist PAM-4 for datacenter IM-DD optics: An air comparison under practical bandwidth limits," *J. Lightw. Technol.*, vol. 40, no. 10, pp. 3347–3357, May 2022.

[11] M. S. Alam, E. Berikaa, and D. V. Plant, "Net 350 Gbps/λ IMDD transmission enabled by high bandwidth thin-film lithium niobate MZM," *IEEE Photon. Technol. Lett.*, vol. 34, no. 19, pp. 1003–1006, Oct. 2022.

[12] E. Berikaa, M. S. Alam, and D. V. Plant, "Net 400-Gbps/λ IMDD transmission using a single-DAC DSP-free transmitter and a thin-film lithium niobate MZM," *Opt. Lett.*, vol. 47, no. 23, pp. 6273–6276, Dec. 2022.

[13] F. Yang et al., "Monolithic thin-film lithium niobate electro-optic modulator with over 110 GHz bandwidth," *Chin. Opt. Lett.*, vol. 20, no. 2, Feb. 2022, Art. no. 022502.
[14] M. Sakib et al., "A high-speed micro-ring modulator for next generation energy-efficient optical networks beyond 100 Gbaud," in *Proc. Conf. Lasers Electro-Opt.*, 2021, pp. 1–2, Paper SF1C.3.
[15] D. W. U. Chan et al., "C-band 67 GHz silicon photonic microring modulator for dispersion-uncompensated 100 Gbaud PAM-4," *Opt. Lett.*, vol. 47, no. 11, pp. 2935–2938, Jun. 2022.
[16] Y. Zhang et al., "240 Gb/s optical transmission based on an ultrafast silicon microring modulator," *Photon. Res.*, vol. 10, no. 4, pp. 1127–1133, 2022.
[17] O. Ozolins et al., "100 GHz externally modulated laser for optical interconnects," *J. Lightw. Technol.*, vol. 35, no. 6, pp. 1174–1179, Mar. 2017.
[18] J. Wei et al., "Experimental demonstration of advanced modulation formats for data center networks on 200 Gb/s lane rate IMDD links," *Opt. Exp.*, vol. 28, no. 23, pp. 35240–35250, Nov. 2020.
[19] M. S. Bin Hossain et al., "402 Gb/s PAM-8 IM/DD O-band EML transmission," in *Proc. IEEE Eur. Conf. Opt. Commun.*, 2021, pp. 1–4.
[20] M. S. Bin Hossain et al., "Partial response O-band EML transmission beyond 300-GBd with a 128/256 GSa/s DAC," in *Proc. Opt. Fiber Commun. Conf. Exhib.*, 2022, pp. 1–3, Paper M2H.1.
[21] S. Kanazawa et al., "224-Gbit/s 4-PAM operation of a high-modulation-bandwidth high-output-power Hi-FIT AXEL transmitter," *Opt. Lett.*, vol. 47, no. 12, pp. 3019–3022, Jun. 2022.
[22] M. Theurer et al., "200 Gb/s uncooled EML with single MQW layer stack design," in *Proc. Eur. Conf. Opt. Commun.*, 2022, pp. 1–4, Paper Th1E.5.
[23] T. Hiraki et al., "Over-67-GHz-bandwidth membrane InGaAlAs electro-absorption modulator integrated with DFB laser on Si platform," *J. Lightw. Technol.*, vol. 41, no. 3, pp. 880–887, Feb. 2023.
[24] J. M. Estarán et al., "140/180/204-Gbaud OOK transceiver for inter- and intra-data center connectivity," *J. Lightw. Technol.*, vol. 37, no. 1, pp. 178–187, Jan. 2019.
[25] O. Ozolins et al., "Optical amplification-free 200 Gbaud on-off keying link for intra-data center communications," in *Proc. Opt. Fiber Commun. Conf. Exhib.*, 2022, pp. 1–3, Paper Th4A.6.
[26] S. Yamaoka et al., "Directly modulated membrane lasers with 108 GHz bandwidth on a high-thermal-conductivity silicon carbide substrate," *Nature Photon.*, vol. 15, no. 1, pp. 28–35, 2020.
[27] N.-P. Diamantopoulos et al., "$>$100-GHz bandwidth directly-modulated lasers and adaptive entropy loading for energy-efficient $>$300-Gbps/λ IM/DD systems," *J. Lightw. Technol.*, vol. 39, no. 3, pp. 771–778, Feb. 2021.
[28] N.-P. Diamantopoulos et al., "60 GHz bandwidth directly modulated membrane III-V lasers on SiO2/Si," *J. Lightw. Technol.*, vol. 40, no. 10, pp. 3299–3306, May 2022.
[29] S. Yamaoka et al., "Uncooled 100-GBaud operation of directly modulated membrane lasers on high-thermal-conductivity SiC substrate," in *Proc. Eur. Conf. Opt. Commun.*, 2022, pp. 1–4, Paper We1E.3.
[30] Y. Matsui, R. Schatz, D. Che, F. Khan, M. Kwakernaak, and T. Sudo, "Low-chirp isolator-free 65-GHz-bandwidth directly modulated lasers," *Nature Photon.*, vol. 15, no. 1, pp. 59–63, 2020.
[31] D. Che et al., "Long-term reliable $>$200-Gb/s directly modulated lasers with 800GbE-compliant DSP," in *Proc. IEEE Opt. Fiber Commun. Conf. Exhib.*, 2021, pp. 1–3.
[32] A. Shams-Ansari et al., "Electrically pumped laser transmitter integrated on thin-film lithium niobate," *Optica*, vol. 9, no. 4, pp. 408–411, Apr. 2022.
[33] "Concatenated FEC proposal for 200G/lane PMD." Accessed: Dec. 19, 2022. [Online]. Available: https://www.ieee802.org/3/df/public/22_05/22_0518/patra_3df_01_220518.pdf
[34] "800G-FR4 technical specification," 2021. [Online]. Available: https://www.800gmsa.com/
[35] "Coherent introduces 200G indium phosphide electro-absorption modulated lasers for high-speed datacenter transceivers," 2022. Accessed: Feb. 10, 2023. [Online]. Available: https://www.coherent.com/news/press-releases/coherent-introduces-200g-indium-phosphile-electro-absorption-modulated-lasers
[36] "Broadcom's 100Gbps VCSEL and 200Gbps EML enable next-generation 1.6Tbps pluggable optics," 2022. Accessed: Feb. 10, 2023. [Online]. Available: https://www.broadcom.com/blog/100gbps-vcsel-and-200gbps-eml-enable-next-generation-pluggable-optics
[37] "Lumentum: 200G PAM4 externally modulated lasers (EMLs)," 2023. Accessed: Feb. 10, 2023. [Online]. Available: https://www.lightwaveonline.com/optical-tech/components/article/14289296/lumentum-200g-pam4-externally-modulated-lasers-emls
[38] X. Pang et al., "200 Gb/s unamplified IM/DD transmission over 20-km SMF with an O-band low-chirp directly modulated laser," in *Proc. IEEE Eur. Conf. Opt. Commun.*, 2022, pp. 1–4.
[39] L. M. Zhang and F. R. Kschischang, "Staircase codes with 6% to 33% overhead," *J. Lightw. Technol.*, vol. 32, no. 10, pp. 1999–2002, May 2014.
[40] U. Feiste, "Optimization of modulation bandwidth in DBR lasers with detuned Bragg reflectors," *IEEE J. Quantum. Electron.*, vol. 34, no. 12, pp. 2371–2379, Dec. 1998.
[41] M. Chaciński and R. Schatz, "Impact of losses in the Bragg section on the dynamics of detuned loaded DBR lasers," *IEEE J. Quantum Electron.*, vol. 46, no. 9, pp. 1360–1367, Sep. 2010.